JACS
JOURNAL OF THE AMERICAN CHEMICAL SOCIETY
Communication
pubs.acs.org/JACS

# Porphyrin Triplet State as a Potential Spin Label for Nanometer Distance Measurements by PELDOR Spectroscopy

Marilena Di Valentin,* Marco Albertini, Enrico Zurlo, Marina Gobbo, and Donatella Carbonera

Dipartimento di Scienze Chimiche, Università di Padova, via Marzolo 1, 35131 Padova, Italy

Supporting Information

**ABSTRACT:** This work demonstrates, for the first time, the feasibility of applying pulsed electron−electron double resonance (PELDOR/DEER) to determine the interspin distance between a photoexcited porphyrin triplet state ($S = 1$) and a nitroxide spin label chemically incorporated into a small helical peptide. The PELDOR trace shows deep envelope modulation induced by electron−electron dipole interaction between the partners in the pair, providing an accurate distance measurement. This new labeling approach has a high potential for measuring nanometer distances in more complex biological systems due to the sensitivity acquired from the spin polarization of the photoexcited triplet state spectrum.

Pulsed electron−electron double resonance (PELDOR/DEER) is a powerful and well-established methodology for measuring nanometer distances in spin-labeled systems.[1−5] PELDOR spectroscopy can probe, from measurements of the electron−electron dipolar interaction between the two paramagnetic centers, their separation and relative orientation according to eq 1, in which $g_1$ and $g_2$ are the $g$-factors for the two spin systems, $r$ is the interspin distance, and $\theta$ is the angle between the spin−spin vector and the external magnetic field.

$$\nu_{DD}(r, \theta) = \frac{g_1 g_2 \beta_e^2 \mu_0}{4\pi h r^3}(3\cos^2\theta - 1) \quad (1)$$

Conventionally, PELDOR measurements are performed between two nitroxide spin labels which have been attached to biological molecules either by site-directed spin labeling or by chemical modification.[6] In recent years, numerous efforts have been devoted to the development of alternative spin labels, featuring more attractive properties than conventional nitroxide radicals, despite their widespread employment for distance measurements.

The orthogonal labeling approach, based on the use of spectroscopically nonidentical labels, which can be addressed selectively in the electron paramagnetic resonance (EPR) experiment, has proved to be very promising for the Gd(III)−nitroxide pair, inserted in both model systems and proteins and featuring a high sensitivity at high-field EPR.[7−9]

Also promising are the recent technological advances in high-field PELDOR, which enable orientationally selective experiments, thus providing the possibility to unravel the relative orientation of spin labels and yielding considerably more structural information.[10,11] For this reason and in order to exploit endogenous probes, PELDOR spectroscopy using paramagnetic metal cofactors has been tentatively performed not only on model systems but also on various classes of metalloproteins and proteins with metal-based spin tags at specific sites. A limited number of examples has been reported to date, restricted to metal centers exhibiting small anisotropy of the $g$-tensor and relatively slow relaxation times. These are $S = 1/2$ systems or high-spin systems for which mainly the $\Delta m = \pm 1/2$ transition can be selected, i.e., Cu(II), iron−sulfur centers, the above-mentioned Gd(III), Mn(II), and Mn clusters.[12−23] Recently, the feasibility of PELDOR experiments between nitroxide spin labels and low-spin ferric heme centers has been demonstrated.[24]

Further development of orthogonal labeling approaches is thus essential to broaden the applicability of this powerful spectroscopic technique. In this work, we explore the possible advantage of using a photoexcited triplet state ($S = 1$), localized on a porphyrin moiety, as an orthogonal spin label to be coupled to the nitroxide radical.

The triplet state has distinctive properties compared to metal centers, since the large anisotropy due, in the specific case, to the zero-field splitting (ZFS) tensor is accompanied by a strong spin polarization of the spectrum,[25] resulting from a non-Boltzmann population of the triplet-state sublevels by intersystem crossing from the corresponding excited singlet state. Among organic chromophores, porphyrins have been widely studied by EPR spectroscopy, due to their high triplet yields, strong spin polarization, nonextreme relaxation times, and moderate spectral anisotropy caused by the ZFS interaction.[26]

To verify the feasibility of measuring nitroxide−porphyrin triplet state interspin distances, we have designed a bis-labeled model peptide with well-defined, predictable separations between the paramagnetic sites (Figure 1). The 15-residue peptide is labeled at the N-terminal end with 5-(4-carboxyphenyl)-10,15,20-triphenylporphyrin (TPP) and at position 10 with 4-amino-1-oxyl-2,2,6,6-tetramethylpiperidine-4-carboxylic acid (TOAC).

The peptide bridge connecting the paramagnetic probes consists of alternating L-alanine (Ala) and $\alpha$-aminoisobutyric acid (Aib) residues, known to promote the $\alpha$-helix conformation and consequently a well-defined geometry in terms of distance, relative orientation, and restricted conformational flexibility.[27]

**Received:** March 14, 2014
**Published:** April 15, 2014

   dx.doi.org/10.1021/ja502615n | J. Am. Chem. Soc. 2014, 136, 6582−6585

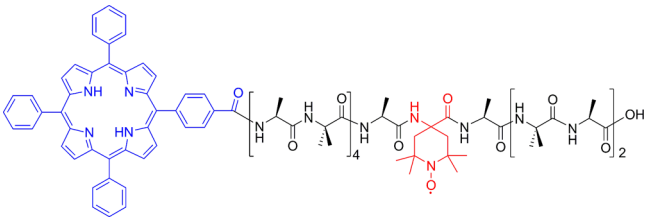

**Figure 1.** Chemical structure of the bis-labeled peptide TPP-(Ala-Aib)$_4$-Ala-TOAC-Ala-(Aib-Ala)$_2$-OH.

Syntheses of the (Ala-Aib)$_n$ sequence and its TOAC-containing analogue were performed by standard solid-phase synthesis, following a protocol previously optimized for spin-label-containing peptides.[28] 5-(4-Carboxyphenyl)-10,15,20-triphenylporphyrin was covalently linked to the N-terminus of the TOAC-containing peptide, still attached to the solid support, in the presence of *N,N′*-diisopropylcarbodiimide/1-hydroxybenzotriazole in $CH_2Cl_2$/DMF. Cleavage of the porphyrin–peptide conjugate from the resin was achieved by a mild acidic treatment that prevents the loss of the spin label by protonation. TPP-(Ala-Aib)$_4$-Ala-TOAC-Ala-(Aib-Ala)$_2$-OH was characterized by analytical HPLC, UV–Vis and FT-IR spectroscopies, and ESI-MS. Circular dichroism (CD) was used to assess that, in methanol, the solvent used for the EPR measurements, the labeled peptide retains the $\alpha$-helical structure of the parent peptide (see Figure S1 in the Supporting Information (SI)). From CD, self-aggregation was also excluded.

The pulsed EPR measurements were carried out at X-band with a wide-bandwidth split-ring resonator on a glassy frozen solution (20 K) of the compound in perdeuterated methanol at a concentration of ~200 $\mu$M. A laser flash at 532 nm, used to populate the TPP triplet state, is followed by the microwave pulse sequences corresponding to the electro-spin echo and four-pulse PELDOR experiments (experimental details in SI).

In Figure 2, top panel, the photoexcited field-swept electron-spin echo spectrum of the TPP-conjugated model peptide is depicted, which shows the narrow central absorption signal due to the nitroxide spin label (enlargement of the corresponding spectral region is reported in the inset, detected in the absence of laser photoexcitation) and the broad contribution, extending between 300 and 380 mT, due to TPP triplet state.

The triplet state spectrum displays turning points corresponding to the canonical orientations of the anisotropic ZFS tensor and a specific spin-polarization pattern composed by enhanced absorptive (A) and emissive (E) lines, as a result of a non-Boltzmann population of the triplet-state sublevels. The detailed spectroscopic characterization of the TPP triplet state is reported in the SI (see Figure S2 and Table S1).

Figure 2, bottom panel, depicts the four-pulse PELDOR time trace, obtained by applying the pump pulse at the maximum of the nitroxide spectrum, in order to optimize the pump efficiency, and the observer sequence in correspondence to the most intense emissive ZFS canonical transition of the polarized TPP triplet state spectrum, generated via pulsed laser excitation. The PELDOR trace reveals a well-resolved and pronounced dipolar modulation and a weak damping, up to at least five complete periods. The modulation stems from dipolar coupling of spin pairs with a single dominating distance. This behavior is characteristic of restricted conformational flexibility and distance distribution of the spin probes.

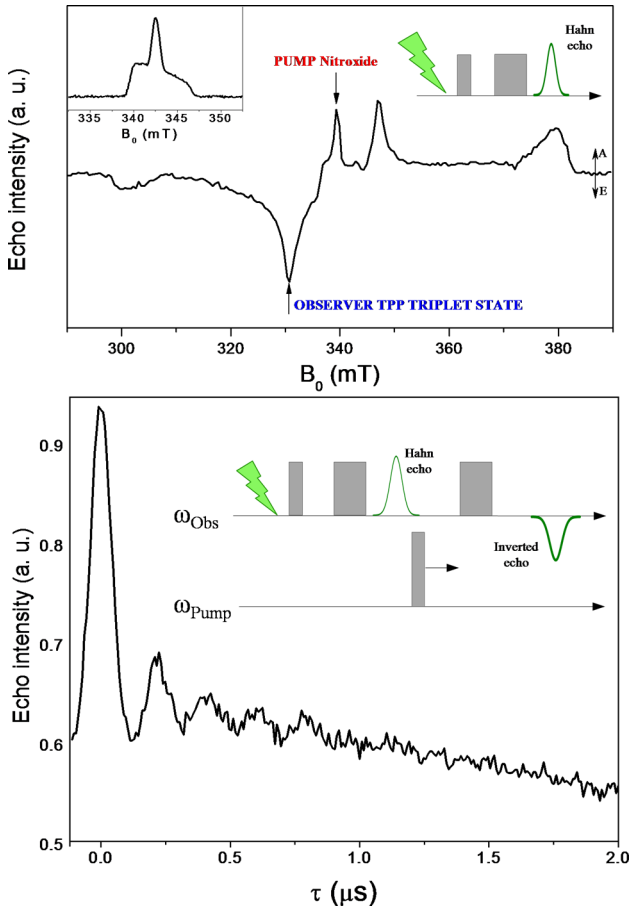


**Figure 2.** Top panel: X-band field-swept electron-spin echo spectrum of TPP-(Ala-Aib)$_4$-Ala-TOAC-Ala-(Aib-Ala)$_2$-OH (~200 $\mu$M) recorded under photoexcitation at 20 K. A two-pulse echo sequence ($\pi/2-\tau-\pi$) was used with a 16 ns $\pi/2$ pulse and $\tau$ = 300 ns. The inset depicts the spectrum of the nitroxide label in the absence of laser photoexcitation. The arrows indicate the positions of pumping (nitroxide) and detection (TPP triplet state) in the PELDOR experiment shown in the bottom panel. A = enhanced absorption, E = enhanced emission. Bottom panel: X-band four-pulse PELDOR trace recorded under photoexcitation at 20 K. Observer pulses 16/32/32 ns, pump pulse 12 ns, $\Delta\nu$ = 240 MHz, shots per point = 50, and single scan.

Optimization of the time trace in terms of signal-to-noise ratio was achieved by reducing by 100 times the number of scans compared to typical measurements in nitroxide–nitroxide PELDOR experiments. The significantly increased sensitivity is due to the intrinsic spin polarization, which is only partially lost in the broad features of the triplet-state spectrum. Moreover, the phase memory time of the triplet state at cryogenic temperatures is comparable to that of nitroxide spin labels in the conditions commonly adopted for PELDOR measurements (see Figure S3 for data recorded to assess phase memory time).

To verify that the detected modulation originates from electron–electron dipole interaction between the $S$ = 1/2 and $S$ = 1 partners, we performed control PELDOR experiments with different settings of the pump and observer frequency. Indeed, by choosing both the pump field and the observer field within the nitroxide or the porphyrin spectrum, we observed no modulation but only an exponential decay corresponding to the homogeneous distribution of peptides in the glassy frozen solution (data not shown).


dx.doi.org/10.1021/ja502615n | J. Am. Chem. Soc. 2014, 136, 6582–6585

After removal of the background decay from the envelope modulation, Fourier transformation of the signal provides the frequency spectrum reported in Figure 3, in which the maximum intensity is observed at the dipolar frequency $\nu_{DD}$ = 4.8 MHz. Although a significant extent of orientation selection is expected in the relatively broad porphyrin triplet spectrum, the effect is not visible on the PELDOR spectrum, showing the shape of a pake pattern. This is because at the observer position almost all the possible molecular orientations with the tetrapyrrole plane parallel to the magnetic field are detected. The orientation selection is further compromised by the lack of collinearity between the ZFS principal axes and the spin−spin distance vector, according to the structural model, and to a lesser extent by the small degree of rotational freedom of the para-substituted benzoyl group with respect to the $C^1_{phenyl}$−CO and the $C^4_{phenyl}$−tetrapyrrole ring bonds (structural details reported in Figure S4).

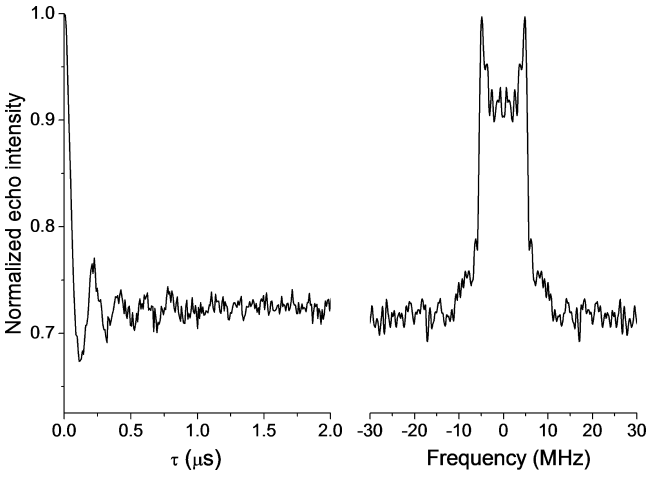


**Figure 3.** Left: X-band four-pulse PELDOR trace of TPP-$(Ala\text{-}Aib)_4$-Ala-TOAC-Ala-$(Aib\text{-}Ala)_2$-OH after background removal. Right: Fourier transform of the time domain trace after background removal.

An interspin distance of 22.4 Å was derived from eq 1, applicable to the triplet state according to ref 29, in the high-field approximation and neglecting any contribution from the exchange interaction at this large distance between the spin systems. Small deviations from this value might derive also from the ZFS contribution to the spin Hamiltonian.[18,30,31] Despite these limits, the estimated distance is consistent with the one obtained in the point-dipole approximation from the structural model of TPP-$(Ala\text{-}Aib)_4$-Ala-TOAC-Ala-$(Aib\text{-}Ala)_2$-OH, considering the spin label positions with the center of the porphyrin macrocycle and the midpoint of the nitroxide N−O bond as reference points in the calculation (reported in Figure S4 together with the distance distribution obtained with DeerAnalysis2013 software[32]).

This result demonstrates the feasibility of using PELDOR spectroscopy to determine the interspin distance between nitroxide spin labels and porphyrin triplet states and opens new possibilities for investigating the structure of biomolecules exploiting the triplet state. This is the first example of PELDOR based on a photoexcited $S > 1/2$ spin label.

Porphyrin triplet states have a potential for application as novel spin labels. They feature high sensitivity, exceeding that of the nitroxide−nitroxide PELDOR, due to the high spin polarization while displaying phase and spin−lattice relaxation times comparable to those nitroxides.

Porphyrin triplet states work very efficiently as orthogonal labels, adding to the spectroscopic selectivity to nitroxide the advantage of behaving as photoinduced spin probes. This feature reveals intermolecular interactions and oligomerization states, in the same sample, by performing PELDOR in the absence of light excitation to measure intermolecular nitroxide−nitroxide distances. Moreover, the well-characterized optical properties of the porphyrin chromophore can be exploited to combine PELDOR to the complementary Förster resonance energy transfer (FRET) spectroscopic method using a common label, i.e., the porphyrin, which is fluorescent and paramagnetic at the same time, while replacing the nitroxide by a suitable FRET partner.

This study opens new promising possibilities for investigating the structure of biomolecular assemblies. Application to proteins containing heme groups, which can be Zn-substituted in order to populate the Zn(II) protoporphyrin IX triplet state,[33] can be foreseen. For a more general purpose, site-specific spin-labeling of proteins using developed protocols can be extended to bind the porphyrin moiety in selected sites suitably chosen.[6] In addition, this type of orthogonal approach can be extended to other chromophores whose triplet state is highly polarized and well-characterized by EPR spectroscopy, like porphyrin derivatives, fullerenes, and flavins.[34−37] In particular, chlorophylls and flavins can be exploited as endogenous probes because of their presence in several classes of proteins. Furthermore, the strong anisotropy of the triplet-state ZFS tensor, which produces a spectral width similar to that of high-spin metal centers, can be potentially exploited to perform orientation selection taking advantage of the compensating effect of the spin polarization signal enhancement.

We are currently exploring the practical limits of the four-pulse PELDOR experiment for the determination of distance distributions on the nitroxide−photoexcited triplet state spin label pair using a porphyrin-based peptide molecular ruler.

## ■ ASSOCIATED CONTENT

### Ⓢ Supporting Information

Synthesis and characterization of the bis-labeled model peptide; CD spectra; descriptions of sample preparation and EPR experiments; time-resolved and pulsed EPR data. This material is available free of charge via the Internet at http://pubs.acs.org.

## ■ AUTHOR INFORMATION

### Corresponding Author

marilena.divalentin@unipd.it

### Notes

The authors declare no competing financial interest.

## ■ ACKNOWLEDGMENTS

The authors thank Prof. F. Formaggio for helpful discussions. Financial support from MIUR (PRIN2010-2011 prot. 2010FM38P_004 and Cariparo Foundation (M3PC project) is gratefully acknowledged.

## ■ REFERENCES

(1) Jeschke, G.; Pannier, M. M.; Spiess, H. W. In *Distance Measurements in Biological Systems by EPR*; Berliner, L. J., Eaton, S. S., Eaton, G. R., Eds.; Kluwer Academic: New York, 2000; Vol. *19*, pp 493−512.

(2) Schiemann, O.; Prisner, T. F. *Q. Rev. Biophys.* **2007**, *40*, 1.
(3) Tsvetkov, Y. D.; Milov, A. D.; Maryasov, A. G. *Russ. Chem. Rev.* **2008**, *77*, 487.
(4) Reginsson, G. W.; Schiemann, O. *Biochem. J.* **2011**, *434*, 353.
(5) Jeschke, G. *Annu. Rev. Phys. Chem.* **2012**, *63*, 419.
(6) Klare, J. P.; Steinhoff, H.-J. *Photosynth. Res.* **2009**, *102*, 377.
(7) Kaminker, I.; Yagi, H.; Huber, T.; Feintuch, A.; Otting, G.; Goldfarb, D. *Phys. Chem. Chem. Phys.* **2012**, *14*, 4355.
(8) Kaminker, I.; Tkach, I.; Manukovsky, N.; Huber, T.; Yagi, H.; Otting, G.; Bennati, M.; Goldfarb, D. *J. Magn. Reson.* **2013**, *227*, 66.
(9) Lueders, P.; Jäger, H.; Hemminga, M. A.; Jeschke, G.; Yulikov, M. *J. Phys. Chem. B* **2013**, *117*, 2061.
(10) Milikisyants, S.; Groenen, E. J. J.; Huber, M. *J. Magn. Reson.* **2008**, *192*, 275.
(11) Goldfarb, D.; Lipkin, Y.; Potapov, A.; Gorodetsky, Y.; Epel, B.; Raitsimring, A. M.; Radoul, M.; Kaminker, I. *J. Magn. Reson.* **2008**, *194*, 8.
(12) Narr, E.; Godt, A.; Jeschke, G. *Angew. Chem., Int. Ed.* **2002**, *41*, 3907.
(13) van Amsterdam, I. M. C.; Ubbink, M.; Canters, G. W.; Huber, M. *Angew. Chem., Int. Ed.* **2003**, *42*, 62.
(14) Kay, C. W. M.; El Mkami, H.; Cammack, R.; Evans, R. W. *J. Am. Chem. Soc.* **2007**, *129*, 4868.
(15) Bode, B. E.; Plackmeyer, J.; Bolte, M.; Prisner, T. F.; Schiemann, O. *J. Organomet. Chem.* **2009**, *694*, 1172.
(16) Lovett, J. E.; Bowen, A. M.; Timmel, C. R.; Jones, M. W.; Dilworth, J. R.; Caprotti, D.; Bell, S. G.; Wong, L. L.; Harmer, J. *Phys. Chem. Chem. Phys.* **2009**, *11*, 6840.
(17) Elsässer, C.; Brecht, M.; Bittl, R. *J. Am. Chem. Soc.* **2002**, *124*, 12606.
(18) Raitsimring, A. M.; Gunanathan, C.; Potapov, A.; Efremenko, I.; Martin, J. M. L.; Milstein, D.; Goldfarb, D. *J. Am. Chem. Soc.* **2007**, *129*, 14138.
(19) Yagi, H.; Banerjee, D.; Graham, B.; Huber, T.; Goldfarb, D.; Otting, G. *J. Am. Chem. Soc.* **2011**, *133*, 10418.
(20) Matalon, E.; Huber, T.; Hagelueken, G.; Graham, B.; Frydman, V.; Feintuch, A.; Otting, G.; Goldfarb, D. *Angew. Chem., Int. Ed.* **2013**, *125*, 12047.
(21) Garbuio, L.; Bordignon, E.; Brooks, E. K.; Hubbell, W. L.; Jeschke, G.; Yulikov, M. *J. Phys. Chem. B* **2013**, *117*, 3145.
(22) Banerjee, D.; Yagi, H.; Huber, T.; Otting, G.; Goldfarb, D. *J. Phys. Chem. Lett.* **2012**, *3*, 157.
(23) Asada, M.; Nagashima, H.; Koua, F. H. M.; Shen, J.-R.; Kawamori, A.; Mino, H. *Biochim. Biophys. Acta Bioenerg.* **2013**, *1827*, 438.
(24) Ezhevskaya, M.; Bordignon, E.; Polyhach, Y.; Moens, L.; Dewilde, S.; Jeschke, G.; Van Doorslaer, S. *Mol. Phys.* **2013**, *111*, 2855.
(25) Lubitz, W.; Lendzian, F.; Bittl, R. *Acc. Chem. Res.* **2002**, *35*, 313.
(26) van der Waals, J. H.; van Dorp, W. G.; Schaafsma, T. J. In *The Porphyrins*; Dolphin, D., Ed.; Academic Press Inc.: New York, 1979; Vol. *IV*, pp 257−312.
(27) Arikuma, Y.; Nakayama, H.; Morita, T.; Kimura, S. *Angew. Chem., Int. Ed.* **2010**, *49*, 1800.
(28) Gobbo, M.; Merli, E.; Biondi, B.; Oancea, S.; Toffoletti, A.; Formaggio, F.; Toniolo, C. *J. Pept. Sci.* **2012**, *18*, 37.
(29) Borovykh, I. V.; Kulik, L. V.; Dzuba, S. A.; Hoff, A. J. *J. Phys. Chem. B* **2002**, *106*, 12066.
(30) Yulikov, M.; Lueders, P.; Warsi, M. F.; Chechik, V.; Jeschke, G. *Phys. Chem. Chem. Phys.* **2012**, *14*, 10732.
(31) Potapov, A.; Song, Y.; Meade, T. J.; Goldfarb, D.; Astashkin, A. V.; Raitsimring, A. *J. Magn. Reson.* **2010**, *205*, 38.
(32) Jeschke, G.; Chechik, V.; Ionita, P.; Godt, A.; Zimmermann, H.; Banham, J.; Timmel, C. R.; Hilger, D.; Jung, H. *Appl. Magn. Reson.* **2006**, *30*, 473.
(33) Hoffman, B. M. *J. Am. Chem. Soc.* **1975**, *97*, 1688.
(34) Kay, C. W. M.; Di Valentin, M.; Möbius, K. *Sol. Energy Mater. Sol. Cells* **1995**, *38*, 111.
(35) Angerhofer, A. In *Chlorophylls*; Scheer, H., Ed.; CRC Press: Boca Raton, FL, 1990; pp 945−991.
(36) Franco, L.; Toffoletti, A.; Maggini, M. *Phys. Chem. Chem. Phys.* **2012**, *14*, 14358.
(37) Schleicher, E.; Weber, S. In *EPR Spectroscopy: Applications in Chemistry and Biology*; Drescher, M., Jeschke, G., Eds.; Springer-Verlag: Berlin, 2012; Vol. *321*, pp 41−65.